Current Botany 2024, 15: 138-150
doi: 10.25081/cb.2024.v15.9139
https://updatepublishing.com/journal/index.php/cb

Research Article

ISSN: 2220-4822

Titanium dioxide (TiO_2) nanoparticles improved morpho-physiological characters and DNA content in *Swietenia macrophylla* an IUCN red listed endangered plant species

Deepak Kumar Verma[1]*, Alpesh B. Thakor[1], Sapan Patel[2]

[1]Biology Department, B.K.M. Science College, Valsad, Veer Narmad South Gujarat University, Surat-395007, Gujarat, India, [2]School of Studies in Botany, Jiwaji University, Gwalior-474011, Madhya Pradesh, India

ABSTRACT

There is a great need to improve plant resilience to unpredictable environmental stresses; therefore, understanding the leading role of Titanium dioxide (TiO_2) nanoparticles in alleviating plant stress is crucial for the development of abiotic stress-tolerant endangered plant species. Recently, many new methods have emerged to synthesize nanoparticles, among which the biosynthesis method deserves more attention due to its features such as being eco-friendly, and cost-efficient. The aim of the present study is to perform green synthesis of nanoparticles from extracts and investigate the effect of these nanoparticles on plants. The complete shape and size of the synthesized nanoparticles were analyzed by UV-visible spectroscopy (UV-Vis), Particle Size Analysis (PSA), Fourier Transform Infrared Spectroscopy (FTIR), X-Ray Diffraction (XRD), Scanning Electron Microscopy (SEM) modern instruments. The absorption peak at 310 nm wavelength obtained from UV–Visible spectroscopy analysis confirmed the synthesis of TiO_2 nanoparticles (NPs). The presence of strong and broad peaks in FTIR indicated the presence of phytochemicals functional groups and the presence of NPs. SEM result showed that most of the synthesized nanoparticles had spherical angular structure and their size was 75 nm. The effects of TiO_2 NPs on *Swietenia macrophylla* L. an endangered plant species listed in IUCN (International Union for Conservation of Nature) showed that seed germination and plant survival rates were higher than control plants and there was also significant variation in root and shoot development and growth of leaves. The growth rate of the plants was significant compared to control and the chlorophyll pigments content was also recorded significant in the treated plants. The 21 phytochemicals were identified in the plant leaves analyzed with GC-MS. The ISSR analysis result showed polymorphic DNA a band which was as mutants in phenotypic characters of plants. Flow cytometric results had shown that DNA replicate content was increased due to TiO_2 NPs effect in plants treated with 200 mgL^{-1} showed the higher plant growth efficiency.

KEYWORDS: Chlorophylls, Cytometry, Gas Chromatography Mass Spectrometry, Nanoparticles, Mahogany

Received: September 03, 2024
Revised: October 24, 2024
Accepted: October 27, 2024
Published: November 19, 2024

***Corresponding author:**
Deepak Kumar Verma
E-mail: vermadeepakbotany@gmail.com

INTRODUCTION

Nanobiotechnology has profoundly transformed science and plays a major role in many new aspects of the new millennium. Particularly compared to bulk materials, nanoparticles (NPs) have distinct physical, chemical, and biological properties depending on their quality. It is always widely believed that the fundamental properties of nanostructured materials depend on their size and shape. Metallic nanoparticles are one of the most ubiquitously and multifunctional types of nanomaterials, found in electronics, chemistry, catalysis, and medicine and pharmaceutical applications (Chandren & Rusli, 2022). Over the past few years, nanotechnology has become an emerging tool and an important and innovative proposition in the agricultural industry in areas such as crop production, disease diagnosis, soil improvement, plant breeding, and stress tolerance. More in-depth studies are needed regarding the effects and absorption mechanisms of TiO_2 NPs on specific plant species, since soil is one of the major sinks that receive many of the NPs released in environmental conditions (Metwally *et al.*, 2023).

The mechanisms by which metallic nanoparticles interact with plants at the cellular and molecular levels were also investigated,

as well as the potential applications of bio-based nanoparticles in plant improvement, such as improving nutrient absorption pathway, enhancing abiotic stress tolerance, and promoting sustainable production (Verma *et al.*, 2024). Nano TiO_2 exhibits significantly enhanced photo-catalytic efficiency due to its effective active sites and high surface-to-volume ratio, wide band gap of 3.2 eV easily absorbs ultraviolet light, a feature that promotes strong molecular interactions in plant cells. TiO_2 NPs have the potential to act as interaction agents with several chemical modifications to optimize their biocidal properties. The synthesis of TiO_2 NPs in anatase and rutile forms is widely accepted (Verma *et al.*, 2020b; Sagadevan *et al.*, 2022). It reduces the volatility of substances and can increase their retention time, maintain stability during absorption, improve antioxidant capacity, and prevent inactivation and harmful reactions due to interactions between substance molecules (Huang *et al.*, 2022). The nanostructure of TiO_2 it is possible to reduce or eliminate their toxic properties (cytotoxic and genotoxic), this is similar to preventing the disintegration of nanomaterials due to the release of metal ions (Kushwah & Verma, 2021; Pulit-Prociak *et al.*, 2023).

TiO_2 NPs can be synthesized using several methods, including sol-gel, laser ablation, deposition, hydrothermal, microwave-assisted, and oxidation methods. The plant based synthesis of titanium dioxide NPs has attracted widespread attention among the researchers due to its cheap and cost-effective, eco-friendly method. Green synthesis method of nanoparticles with the help of plants has many advantages, plant extracts act as both reducing and stabilizing agents at the same time and such method also reduces the use of various hazardous chemicals and uses natural substances, which further reduces the toxicity level of TiO_2 nanoparticles (Verma *et al.*, 2021; Yitagesu *et al.*, 2023).

The use of nano-sized TiO_2 on tomato plants increased chlorophyll, and showed a positive correlation with the rate of photosynthesis resulting in improved growth of tomato plants and increased yield. The use of nano-sized TiO_2 increases the levels of P and K in fruits and also enhances the nutritional composition of the stalk juice. However, the use of nano TiO_2 changes the amount of Fe, Zn and B and causes significant changes in the fruit content (Pérez-Velasco *et al.*, 2023; Rathore *et al.*, 2023). Internalization of TiO_2 NPs in *Mentha arvensis* plant parts causes damage to cellular structure. TiO_2 NPs alter micro and nutrient content, biomass pigments due to intracellular oxidative burst in leaves as a result of intracellular ROS generated by TiO_2 NPs. TiO_2 NPs modified the major components of the essential oil of *M. arvensis* from commercially grown plants in contaminated areas. The excessive use of TiO_2 NPs in agricultural technologies needs to be addressed due to their potential biotoxicity (Kumar *et al.*, 2023). Plant metabolites play an important role in plant fitness and adaptation. Therefore, changes in metabolites by TiO_2 NPs affect plant quality (Selvakesavan *et al.*, 2023).

The application of TiO_2 has potential in enhancing pollen viability and fruit quality, which is helpful in developing high quality nano-enabled agriculture (Huang *et al.*, 2022). *Swietenia macrophylla* (Meliaceae family), commonly known as mahogany, is one of the most important timber resources and an economically important tree species, propagated from seeds that lose their viability within a short period of time, making seed germination a critical step for the expansion of the species in India and America, and most valuable in Mexico. The chemical, physical, mechanical and physiological properties of its wood indicate its high economic value (Li *et al.*, 2024). It is in great demand in the international market of the United States, Japan and Europe for plywood and boards, houses, boats and fine cabinet construction. The bioactive compounds limonoids present in its boards, seeds and bark are used in antifungal antibacterial products. Its regeneration and biological mechanism is through seed production, but it depends on the variability of those biological systems and their ability to withstand climate change which is threatening the development of forest areas of biological systems (Wang *et al.*, 2019). It allows free circulation of air which helps in wide spread of seeds. Germination is the most crucial stage of plant growth and temperature is one of the most important environmental factors which controls the maximum percentage of germination.

Mahogany is a tropical hardwood and is used in the manufacturing of cabinetry, furniture, flooring, and musical instruments due to its durability, stability, and beautiful reddish-brown color. *S. macrophylla* contains high amounts of bioactive compounds such as phenols, terpenoids, flavonoids, and alkaloids, which have abundant traditional medicinal properties (Sampayo-Maldonado *et al.*, 2021). *S. macrophylla* exhibits upregulation of mitochondrial apoptosis and colorectal carcinoma cells, the leaves of the plant have antioxidant, antimicrobial, anti-inflammatory, antimutagenic, anti-infective, anti-diabetic, anti-nociceptive, antimalarial, acaricidal, antifeedant and antidiarrheal activity (Sahu *et al.*, 2023). The several bioactive compounds of aqueous extract of *S. macrophylla* leaf have more beneficial effects for human beings. The aqueous extract of leaf has neuroprotective effect in a murine model of Parkinson's disease induced by the 6-hydroxydopamine (6-OHDA), due to the antioxidant and anti-inflammatory properties of the biocompounds (Cardoso *et al.*, 2024). The *S. macrophylla* seeds have high amount of protein (19%) and lipids (71%) have effective biochemicals for controlling of hyperglycemic rats (Jaime *et al.*, 2024).

The aim and objective of this research is to use TiO_2 NPs to improve the intrinsic character and stress tolerance of endangered plants in natural habitat. We synthesized green and eco-friendly TiO_2 NPs from plant species, observed the effect of TiO_2 NPs on seed germination, survival ability, root, shoot growth, photosynthetic pigments, and phytochemicals analysis with GC-MS procedure. The ploidy status of DNA material was observed to improve the genetic characteristics of *S. macrophylla*, a globally endangered plant species. This technique of TiO_2 NPs treatment improves the characteristics of plants and develops resistance to abiotic stresses in their natural habitat.

MATERIALS AND METHODS

Plant and Extract Preparation

Fresh leaves of *Lantana camara* L. were collected in the early morning and washed three times with tap water and distilled water. The fresh leaves were shade dried for a week and ground with an electric grinder. 10 g of leaf powder was placed on filter paper and placed inside a Soxhlet apparatus, 200 mL distilled water was used for aqueous extract extraction at 90 °C for 5 h. After the phytocompounds were completely extracted, the extract was filtered with Whatman filter paper No. 1 and stored in a refrigerator at 4 °C until use. Every process was done separately to avoid contamination.

Synthesis of TiO_2 NPs

TiO_2 NPs were synthesized using leaf extracts with slight modifications to previously reported procedures. The leaf extract acts as both capping and reducing agent, while titanium dioxide powder serves as a precursor for the production of TiO_2 NPs. Firstly, 0.5 mol TiO_2 powder was dissolved in 500 mL distilled water and stirred for 2 h at room temperature. The 50 mL of the remaining extract was stirred in magnetic stirrer at 400 rpm to form the liquid TiO_2 phase. During the reaction, a slight colour change was observed from the precursor colour to a purple and white solid colour, which was obtained after continuous stirring for 8 h. The particles were observed to dissolve completely in the extract for 2 h. The resultant solution was then collected in a petri dish and dried overnight at 60 °C in hot air oven. The dried powder was then crushed with a mortar and pestle and heated in a furnace at 400 °C for 2 h, which transformed the orange coloured powder into a white powder. The resulting TiO_2 NPs were used for further research experiments without any further modification (Rana *et al.*, 2024).

Characterization of TiO_2 Nanoparticles

Several techniques were used to characterize the synthesized TiO2 NPs, such as Particle Size Analysis (PSA) (Malvern Mastersizer 3000), UV-visible spectroscopy (Cary 100 UV-Vis), Scanning Electron Microscopy (SEM) (Zeiss EVO MA10), X-Ray diffraction (XRD) (Mini Flex 600) and Fourier transform Infrared spectroscopy (FTIR) (Vertex 80 FTIR system) (Kushwah & Patel, 2020).

Treatment of Seeds with TiO_2 NPs

Swietenia macrophylla seeds were washed thoroughly in running tap water; subsequently, surface sterilized with sodium hypochlorite (NaOCl) for 5 min, rinsed thoroughly with sterile distilled water, and further used. Different concentrations of TiO_2 nanoparticles were prepared as 25, 50, 100, 200 and 400 mg L^{-1}. Sterilized seeds were kept in different concentrations for 24 hours and sown on filter paper in petri plates. Three replicates were prepared for control and different concentrations of NPs. The 0.5 mL of NPs concentrate was added daily for 7 days (Kushwah *et al.*, 2022). Each concentration had 10 seeds with three replicates. Seeds were tested for germination BOD condition at temperature between 25 °C in the dark. After 10 days root and shoot growth was measured and transferred to the field (soil pH 6.5), plants were analyzed for physical parameters (germination, germination percentage, dead seeds, plant length).

Analysis of Chlorophyll Pigments

Fresh leaves of *S. macrophylla* were collected from 60 day-old plants and washed with tap water and then three times with distilled water. The 0.5 g leaf samples were cut into small pieces and transferred into 10 mL acetone (80%) and crushed using a pestle and mortar. The homogenate was centrifuged at 5000 rpm for 25 min at 4 °C and the supernatant liquid was collected in a test tube and 0.5 mL of it was mixed with 4.5 mL of acetone (80%) solvent. The solutions were analyzed for chlorophyll a, chlorophyll b, and carotenoid content by spectrophotometer (SYSTRONICS Spectrophotometer 169) at three different wavelengths: 663.2, 646.8, and 470 nm (Verma *et al.*, 2020a; Falcioni *et al.*, 2023). The equation used for analyzing chlorophyll content gave the results (given below)

Chlorophyll a = 12.25A663.2−2.79A646.8,

Chlorophyll b = 21.5A646.8−5.1A663.2,

Carotenoids = (1000A470−1.82 Ca − 85.02 Cb) / 198

Where Ca and Cb indicated the concentration of chlorophyll a, b and total carotenoids respectively while A represent the absorption at a given wavelength.

Gas Chromatography Mass Spectroscopy (GC-MS) Analysis of Phytochemicals

Fresh leaves of 120 days old plants were collected from mutant plants treated with NPs at 200 mg L^{-1}, the leaves were shade-dried at room temperature for a week and ground with an electric grinder. The 10 g of *S. macrophylla* leaf powder was weighed and placed in a Soxhlet apparatus with a thimble and 250 mL distilled water at 100 °C for three hours. After mixing, the solution was filtered using a nylon mesh (0.22 micron) and the filtrate was collected. This solution was used for GC-MS (Perkin Elmer Clarus 680) analysis (Pyne & Paria, 2022). The components were identified based on their retention time indices and the mass spectra were interpreted using the National Institute of Standards and Technology (NSIT) database.

ISSR Analysis

Fresh leaves of *S. macrophylla* plants from all the treatment of nanoparticles were collected and washed with tap water to remove dust and debris, then washed three times with double-distilled water. The CTAB method (Li *et al.*, 2022, 2023) was used to isolate the total genomic DNA from the young leaves of *S. macrophylla* plants (1 control, 5 treated plants) which suspected as mutant plants, and the isolated leaves DNA was stored in a deep

refrigerator at -20 °C for further uses. The universal primers UBC 834 (Primer sequences AGAGAGAGAGAGAGAGYT) by UBC (University of British Columbia) for mutant plant screening and genetic diversity was used for the analysis. The protocol 25 µL ISSR-PCR amplification system 12.5 µL 2xPCR Master Mix, 1 µL template DNA, 1 µL primer, and 10.5 µL ddH_2O. The PCR reaction system was pre-denatured at 95 °C for 3 min, denatured at 95 °C for 15 sec, annealed at 61 °C for 15 sec, extended at 72 °C for 1 min, total 32 cycles, and then extended at 72 °C for 5 min to complete the amplification of product and terminate the program at 12 °C. The obtained PCR products were used for gel electrophoresis running for the visualization of the amplified PCR product. The gel was evaluated on the 1.5% agarose gel with 10 µL TS-GelRed Ver.2 Nuclear Staining Dyes and 8 µL of PCR product, and the plate was run in 1× TAE buffer at 150 V for the 20 min. the molecular standered was used 2-log DNA ladder (NEB) After completing electrophoresis, the gel was visualized in the UV transilluminator (Genei) image was taken and analyzed on a gel documentation system (Bio-Rad).

Flow Cytometric Analysis of Leaves

The ploidy status of leaves of *S. macrophylla* was examined using the flow cytometry method described by Galbraith. There were a total of 3 leaf samples, the reference standard was diploid leaves of *S. macrophylla* containing a known amount of 2C DNA of 0.280 pg. 50 mg of leaf was put into a petri plate containing 1.0 mL ice-cold Galbraith buffer (nuclear isolation buffer- 45 mM $MgCl_2$, 20 mM MOPS, 30 mM sodium citrate, 0.1 % (v/v) Triton X-100. Adjust pH to 7.0.) and finely chopped with the help of a surgical blade. The homogenate was filtered through a 100 µm nylon mesh to remove large cellular debris and finally stained with 50 µg/mL PI RNase (propidium iodide RNase) (Sigma-Aldrich) for 8-10 min. Samples were kept in the dark at 4 °C for about 40 min and finally examined on a BD FACS (Calibur) flow cytometer, the relative nuclear DNA of the leaf was estimated using the formula given below- (Bansal *et al.*, 2023).

Nuclear DNA content of sample (pg) = 2C DNA content of standard (pg) × mean position of G0/G1 peak of sample/mean position of G0/G1 peak of standard

Statistical Analysis

Statistical analysis was performed with three replicates. Significant differences between the treated TiO_2 nanoparticles and control groups of plants were tested by one-way variance analysis (ANOVA) with Duncan Multiple Range Test (DMRT) using SPSS statistical software (SPSS Ver. 29.02, IBM US). All data were represented as arithmetic mean±SE (Standard error), ($P \leq 0.05$). The UV-Vis spectra graph analyzed with the software Microsoft 365.

RESULTS

UV-Vis Spectroscopy Analysis of TiO_2 NPs

UV-Vis spectroscopy is a reliable technique for the primary identification of synthesized nanoparticles. It is also used to monitor the synthesis and stability of TiO_2 nanoparticles. Spectrometry makes measurement convenient, it is fast, easy, simple and sensitive to identify the peak absorption of samples within the specified range in a short time and determine the characteristics of suspension particles and the wavelength with the highest absorption was selected as the peak absorption of the sample. The UV-Vis spectra show the absorption peak of TiO_2 NPs near 310 nm. The absorption peak depends on the shape of surface molecules as well as impurities. UV-Vis peaks were obtained in the range of 200-700 nm depending on the size and shape of the synthesized TiO_2 NPs (Figure 1).

Particle Size Analysis of TiO_2 NPs

Size analysis was carried out by particles size analyzer to determine the particle size, the TiO_2-anatase NPs size was uniform and the average particle size was 75 nm. TiO_2 is primarily prepared as powdered anatase using green precursors, which impart unique properties to the particles. Morphology of the particles TiO_2-anatase had nearly spherical particle shape and opaque particles. The TiO_2 NPs particles appear to be elongated possibly due to the growth during the interface nucleation process and phase transition (Figure 2).

Fourier Transform Infrared Spectroscopic analysis of TiO_2 NPs

Fourier transform infrared spectroscopy (FT-IR) is used to detect biomolecules that have a reducing or screening role in ion absorption. FT-IR spectroscopy is a suitable method for detecting bioactive components in biological samples. It is a valuable tool for identifying the presence of secondary metabolites on TiO_2 nanoparticles. The constituent groups present in the NPs were identified using FT-IR spectrometry in the range of 4000-500 cm^{-1}. In the FTIR spectrum of TiO_2 NPs was observed, the NPs peaks showed that broad peak spectra represented at 3349.25 cm^{-1} which indicated that was presence of alcohol intermolecular bonded O–H stretching. The peaks at 1628.43 cm^{-1} are associated with C=C stretching vibrations of conjugated alkene. The 1263.77 peak indicated that the C–O stretching vibration of alkyl aryl ether, and 827.85 cm^{-1} indicated that the C=C bending alkene trisubstituted, these peaks were attributed to the presence of plant extracts in the NPs. The formation of TiO_2 stretching vibrations confirmed

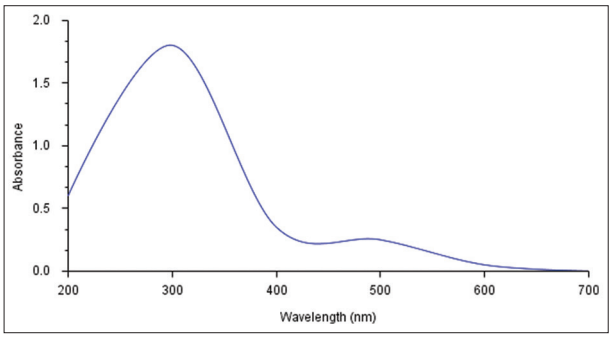

Figure 1: UV-Vis spectroscopy analyzed graph of green synthesized TiO_2 NPs

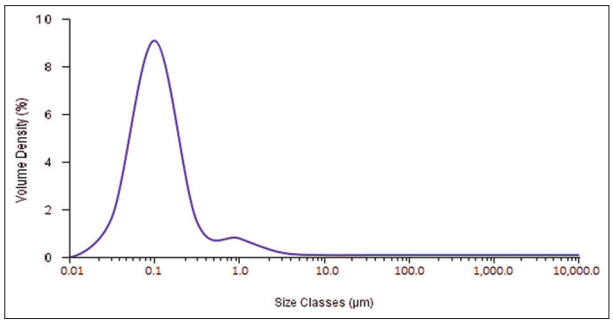

Figure 2: Particle size analyzed graph of green synthesized TiO_2 NPs

the formation of NPs, indicating that the phytochemicals, such as phenols and flavonoids, present in the aqueous extract were responsible for reducing and stabilizing the metal ions to form TiO_2 NPs (Figure 3).

X-ray Diffraction of TiO_2 NPs

X-ray diffraction (XRD) is an analytical technique for analyzing crystal structures, molecular, qualitative identification of crystal compounds, isomorphous, crystalline phase, size and purity of TiO_2 particles. The analysis of nanomaterials depends on the formation of diffraction patterns. All materials have a unique diffraction beam, which was identified using diffraction beams with reference databases and the diffraction patterns indicate the purity of the analyzed samples. X-Ray diffraction peaks at 2θ range of 20°-80°, the XRD pattern of the synthesized TiO_2 NPs exhibits peaks at 11.5°, 23.8°, 32.6°, 37.5°, 43.2°, 51.7°, 68.2° and 65.3° which were corresponding to the (101), (004), (200), (105), (211), (204), (220), (215) refection planes. The indicated XRD pattern crystal structure revealed that the TiO_2 nanoparticles were crystalline in nature anatase phase (Figure 4).

Scanning Electron Microscopy of TiO_2 NPs

Among various analytical techniques of electron microscope, SEM is an electron beam imaging method which is fully capable of identifying the nano scale and surface morphology of synthesized particles of various sizes of nanomaterials. The electron beam to acquire high-quality surface images, and provides various nano-topographical information depending on the electron density of the surface. The size and shape of the TiO_2 NPs was depend on the surface-to-volume ratio and nature of capping agent present in the aqueous plant leaves extract. The SEM micrograph shows the spherical and elliptical size and shape of TiO_2 NPs (Figure 5).

Effect of TiO_2 NPs on Seed Germination and Survival

The 10 seeds of *S. macrophylla* with three replicates (10 × 3 = 30 seeds) were weighed for each treatment, the average weight was 7.4 at control, 100, and 400 mg L^{-1} concentrations, while the average weight was 7.3 at 25, 50, and 200 mg L^{-1} concentrations. At 100 and 200 mg L^{-1} treatments the first seeds germinated on the 5th day, and at 25, 50, and 400 mg L^{-1} they germinated on the 6th day as well as the control seeds. Germination percentage of

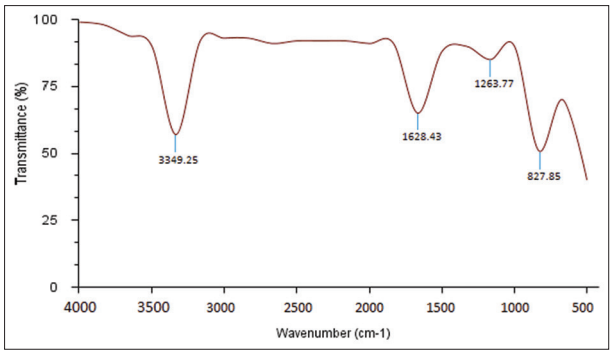

Figure 3: Fourier Transform Infrared Spectroscopy analyzed graph of synthesized TiO_2 NPs

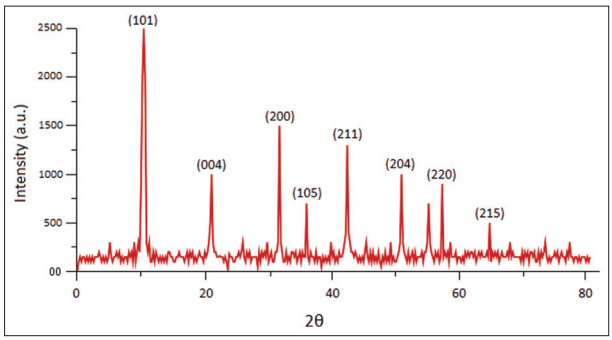

Figure 4: X-ray Diffraction pattern of green synthesized TiO_2 NPs

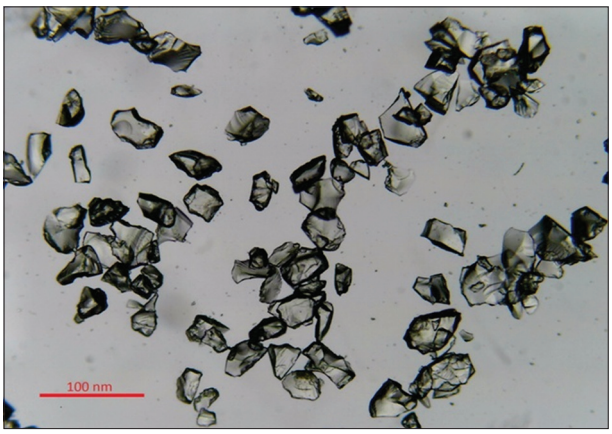

Figure 5: Scanning Electron Microscopy micrograph image of green synthesized TiO_2 NPs

seeds treated with nanoparticles was highest 86.66% at 200 mg L^{-1}, followed by 76.66% at 100 mg L^{-1}, 70.00% at 50 mg L^{-1}, 66.66% at 400 mg L^{-1} and 63.33 at 25 mg L^{-1}, lowest germination value 53.33 was recorded in control. After 10 days all the plants are transferred to black polybags with garden soil in natural habitat for plant growth and development. The seed germination pattern and structure is shown in the (Figure 6 and Table 1).

The survival of germinated seeds was 80.00% at 200 mg L^{-1}, 73.33% at 100 mg L^{-1}, 63.33% at 50 mg L^{-1}, 60.00% at 25 mg L^{-1}, and 56.66% at 400 mg L^{-1} of TiO_2 NPs treatment concentration. The 50.00% survival was in control; all data were recorded after 30 days (Table 1).

Effects of TiO_2 NPs on Root and Seedlings Growth

The data in Table 2 show the effects of different concentrations of TiO_2 NPs on germination, root length, shoot length, and leaf of *S. macrophylla* plants. Initial root growth (10 days) and elongation was observed at 200 mg L^{-1} with maximum of 3.00 cm length. All treatments increased root growth parameters compared to control, the lowest average root length was 1.97 cm recorded in control.

Length of seedlings (20 days) highest length was 7.70 cm at 200 mg L^{-1} NPs treatment, 7.50 cm recorded at 100 mg L^{-1}, 6.70 cm observed at 25 mg L^{-1}, 6.50 cm recorded at 50 mg L^{-1}, and lowest length 5.90 cm at 400 mg L^{-1}, 7.50 cm length of seedling recorded in control. TiO_2 NPs affect shoot growth at 200 mg L^{-1} which is suitable for plant growth rate and development.

Small leaf of (20 days) plants TiO_2 NPs affects the leaf number highest average mean was observed 2.50 at 200 mg L^{-1}, 2.40 recorded at 100 mg L^{-1}, 2.30 recorded at 400 mg L^{-1}, 2.20 recorded at both 25 and 50 mg L^{-1}, lowest average mean value 2.10 observed at control. The TiO_2 NPs were affected and increased leaf growth compared to control seedlings (Table 2).

Figure 6: germination of seeds, root and shoot growth (10 days seedlings) of at different concentrations of TiO_2 NPs a) Control, b) 25 mg L^{-1}, c) 50 mg L^{-1}, d) 100 mg L^{-1}, e) 200 mg L^{-1} and e) 400 mg L^{-1} treatment

Effect of TiO_2 NPs on Plant Growth Rate and Development

The effects of TiO_2 NPs on shoots and leaves of *S. macrophylla* plants are highly influenced by different growth time periods under natural environmental conditions. The shoot length of the plant was recorded in 40 days, shoot length increased significantly 13.40 cm at 200 mg L^{-1} NPs treatment, lowest value was recorded at 10.50 cm at 400 mg L^{-1} treatment, average mean value 11.90 cm recorded at control plants. The number of leaves of plants was observed at 40 days which was significantly increased up to 5.00 at 200 mgL^{-1} NPs treatment, and the lowest average value 3.80 at 25 mg L^{-1} treatment and the average value 3.70 was observed at control which was the lowest compared to all the treatments.

The average value of shoot length of 60 days old plants was increased significantly 20.66 cm at 200 mg L^{-1} treatment, 19.20 cm at 100 mg L^{-1} treatment and the lowest average value 18.00 cm recorded at 400 mg L^{-1} treatment, the average value at control was 18.10 cm. The number of 60 day old leaves was observed in all the treatments, significant increase in number of leaves 6.50 at 200 mg L^{-1} treatment as compared to control, lowest average value recorded 5.30 at 400 mg L^{-1} TiO_2 NPs treatment and average value 5.80 observed at control (Figure 7 and Table 3).

The shoot length of 80 days old plants was observed and significant increase in growth rate with average length 24.50 cm at 200 mg L^{-1} NPs treatment, 24.20 cm at 100 mg L^{-1} treatment, lowest value was 21.80 cm at 400 mg L^{-1} treatment, average

Table 1: Seed weight, seed germination, germination and survival percentage of *S. macrophylla*

Concentrations mg L^{-1}	Seed weight/10 (gm) before sowing	Total number of seeds	Number of germinated seeds	Number of non-germinated seeds	Total germination %	Total survival of seedlings %
Control	7.4	30	16	14	53.33	50.00
25	7.3	30	19	11	63.33	60.00
50	7.3	30	21	09	70.00	63.33
100	7.4	30	23	07	76.66	73.33
200	7.3	30	26	04	86.66	80.00
400	7.4	30	20	10	66.66	56.66

Table 2: Seeds germination in days, root and shoot length and leaves number (average mean±SE, ANOVA, DMRT) of control and treated seedlings of S. *macrophylla*

Concentrations mg L^{-1}	Germination in days	Root length (10 days) cm	Shoot length (20 days) cm	Leaf number (20 days)
Control	6.70 ± 0.21^{b}	1.97 ± 0.07^{a}	7.50 ± 0.26^{bc}	2.10 ± 0.10^{a}
25	6.50 ± 0.16^{b}	2.00 ± 0.06^{a}	6.70 ± 0.30^{ab}	2.20 ± 0.13^{a}
50	6.20 ± 0.20^{ab}	2.00 ± 0.06^{a}	6.50 ± 0.26^{a}	2.20 ± 0.13^{a}
100	5.80 ± 0.20^{a}	2.30 ± 0.08^{a}	7.50 ± 0.30^{bc}	2.40 ± 0.16^{a}
200	5.60 ± 0.22^{a}	3.00 ± 0.10^{a}	$7.70\pm0.26^{c*}$	2.50 ± 0.16^{a}
400	6.10 ± 0.31^{ab}	2.00 ± 0.13^{a}	5.90 ± 0.27^{a}	2.30 ± 0.15^{a}
Sum of sq.	35.650	5.528	66.933	12.183
DF value	59	59	59	59
F value	3.407	0.155	6.423	1.054
Sig.	0.10	0.077	0.001*	0.096

value 23.70 cm recorded in control plants. The 80 days old plants number of leaves also increased significantly average mean value 8.20 recorded at 400 mg L^{-1}, 8.00 at 100 mg L^{-1} and lowest average value 6.90 observed at 400 mg L^{-1} treatment, and 7.80 recorded in control plants.

The height of 100 days old plant was recorded and the growth rate was significant, the average value was 31.00 cm at 200 mg L^{-1} treatment, 30.80 cm measured at 100 mg L^{-1} treatment, the lowest average value recorded 28.80 cm at 400 mg L^{-1} treatment, higher concentrations showed toxic effect on plant height compared to control plants. The mean value in control was recorded as 29.60 cm. The number of leaves of 100 days old plants also increased significantly 11.40 at 200 mg L^{-1} NPs treatment as compared to control, the lowest average value 10.10 recorded at 400 mg L^{-1} NPs treatment which showed toxic effect on plants, average mean value 10.30 recorded in control plants (Table 4).

The height of 120 days old plants was observed and the average value increased significantly to 35.60 cm at 200 mg L^{-1} treatment, 34.40 cm recorded at 100 mg L^{-1} treatment which were the highest respectively compared to the control plants. The lowest average value was recorded at 32.90 cm at 400 mg L^{-1} treatment higher dose had toxicity on plant growth and development compared to control. The average value in control was calculated to be 34.20 cm. The number of leaves of 100 days old plants also increased significantly, the average value 11.70 at 200 mg L^{-1} treatment, the lowest average value 10.20 recorded at 400 mg L^{-1} treatment plants which shows toxic effect compared to control plants, the average value 11.50 in control plants.

Leaf length of 120 days old *S. macrophylla* plants showed significant increase as compared to control plants, average value was recorded as 22.60 cm at 200 mg L^{-1} treatment, 21.90 cm measured at 50 mg L^{-1} NPs treatment, lowest value recorded as 20.40 cm at 400 mgL^{-1} treatment and 21.00 cm measured at control plants. Leaf width of 120 days old mature leaves were measured, the average mean value recorded 6.56 cm at 200 mg L^{-1} treatment which was significantly different than the control plants. Leaf width of all treated plants had increased compared to control plants; the average value of lowest leaf width was 5.95 cm in control plants (Table 5).

Figure 7: The 60 days old *S. macrophylla* plants treated with diffrerent concentrations of TiO_2 NPs a) Control, b) 25 mg L^{-1}, c) 50 mg L^{-1}, d) 100 mg L^{-1}, e) 200 mg L^{-1}, and f) 400 mg L^{-1} treatments

Effects of TiO_2 NPs on Chlorophyll Pigments

Current research involves the effects of TiO_2 NPs on photosynthetic pigments in *S. macrophylla* plant leaves. The analyzed mean values of chlorophyll a, chlorophyll b, carotenoids and total pigments in the leaves of TiO_2 NPs treated and control plant were found to be 1.96, 1.02, 0.77 and 3.75 μg m L^{-1} respectively. Variation was observed in the response of photosynthetic pigments of leaves of *S. macrophylla* plants treated with different concentrations of NPs. The leaves of plants treated with 200 mg L^{-1} treatments showed a greater increase in the content of photosynthetic pigments compared to the control and other concentrations. The average mean values of chlorophyll-a, b, carotenoids, and total pigments increased significantly at 200 mg L^{-1} TiO_2 NPs treatment, which were 2.03, 1.05, 094, and 4.02 μg m L^{-1} respectively. Decreased value of chlorophyll pigment was measured in 400 and 25 mg L^{-1} TiO_2 NPs treatments, growth rate of plants was lower at 400 mg L^{-1} treatment due to high dose of NPs treatment which caused toxicity in plants and inhibited the growth of plants compared to control plants (Table 6).

Gas Chromatography Mass Spectroscopy (GC-MS) Analysis

Gas chromatography mass spectroscopy (GC-MS) analysis identified the presence of secondary metabolites such as

Table 3: Plant height and number of leaves of 40 and 60 days old (average mean±SE, ANOVA, DMRT) of control and treated of *S. macrophylla* plants

Concentrations mg L^{-1}	Plant height 40 days in cm	Leaf number 40 days	Plant height 60 days in cm	Leaf number 60 days
Control	11.90 ± 0.73^{ab}	3.70 ± 0.15^{a}	18.10 ± 0.52^{a}	5.80 ± 0.20^{a}
25	10.90 ± 0.52^{a}	3.80 ± 0.13^{ab}	19.00 ± 0.44^{a}	5.50 ± 0.16^{a}
50	11.20 ± 0.48^{a}	4.20 ± 0.13^{bc}	18.50 ± 0.56^{a}	5.80 ± 0.20^{a}
100	11.70 ± 0.49^{a}	4.50 ± 0.16^{c}	19.20 ± 0.41^{a}	5.70 ± 0.21^{a}
200	$13.40\pm0.49^{b*}$	$5.00\pm0.21^{d*}$	$20.60\pm0.33^{b*}$	$6.50\pm0.16^{b*}$
400	10.50 ± 0.47^{a}	4.60 ± 0.16^{cd}	18.00 ± 0.44^{a}	5.30 ± 0.21^{a}
Sum of sq.	212.400	26.600	161.400	28.733
DF value	59	59	59	59
F value	3.501	9.431	4.305	4.412
Sig.	0.008*	0.001*	0.002*	0.002*

Table 4: Plant height and number of leaves of 80 and 100 days old (average mean±SE, ANOVA, DMRT) of control and treated of *S. macrophylla* plants

Concentrations mg L^{-1}	Plant height 80 days in cm	Leaf number 80 days in cm	Plant height 100 days in cm	Leaf number 100 days in cm
Control	23.70±0.36^{b}	7.80±0.20^{b}	29.60±0.30^{ab}	10.30±0.21^{a}
25	23.80±0.44^{b}	7.60±0.16^{b}	30.10±0.47^{bc}	10.30±0.26^{a}
50	23.20±0.51^{b}	7.80±0.20^{b}	30.10±0.45^{bc}	10.10±0.27^{a}
100	24.20±0.24^{c}	8.00±0.21^{b}	30.80±0.35^{c}	10.30±0.21^{a}
200	24.50±0.54^{bc}*	8.20±0.20^{b}*	31.00±0.33^{c}*	11.40±0.22^{b}*
400	21.80±0.35^{a}	6.90±0.17^{a}	28.80±0.41^{a}	10.10±0.31^{a}
Sum of sq.	164.600	30.183	109.733	46.583
DF value	59	59	59	59
F value	7.527	5.418	4.512	3.783
Sig.	0.001*	0.001*	0.002*	0.005*

Table 5: Plant height and number of leaves, and mature leaf length and width of 120 days old (average mean±SE, ANOVA, DMRT) of control and treated of *S. macrophylla* plants

Concentrations mg L^{-1}	Plant height 120 days in cm	Leaf number 120 days in cm	Mature leaf length in cm	Mature leaf width in cm
Control	34.20±0.24^{b}	11.50±0.22^{b}	21.00±0.29^{ab}	5.95±0.15^{a}
25	33.90±0.37^{ab}	11.70±0.26^{b}	21.60±0.40^{ab}	5.99±0.14^{a}
50	34.30±0.39^{b}	11.40±0.22^{b}	21.90±0.31^{ab}	6.12±0.12^{a}
100	34.40±0.30^{b}	11.30±0.26^{b}	21.40±0.26^{a}	6.24±0.11^{ab}
200	35.60±0.40^{c}*	11.70±0.15^{b}*	22.60±0.37^{b}*	6.56±0.12^{b}*
400	32.90±0.37^{a}	10.20±0.20^{a}	20.40±0.40^{a}	5.98±0.10^{a}
Sum of sq.	106.183	42.600	74.983	11.584
DF value	59	59	59	59
F value	5.990	6.367	1.755	3.298
Sig.	0.001*	0.001*	0.038*	0.011*

Table 6: Effects of different concentrations of TiO_2 NPs on chlorophyll pigment of *S. macrophylla* plants (average mean±SE, ANOVA, DMRT)

Concentrations mg L^{-1}	Chlorophyll-a	Chlorophyll-b	Carotenoid	Total pigments
Control	1.96±0.004^{a}	1.02±0.004^{b}	0.77±0.030^{cd}	3.75
25	1.97±0.003^{a}	1.02±0.006^{b}	0.70±0.029^{bcd}	3.69
50	1.97±0.004^{a}	1.03±0.003^{bc}	0.86±0.016^{d}	3.86
100	1.99±0.013^{ab}	1.04±0.007^{cd}	0.88±0.105^{b}	3.91
200	2.03±0.031^{b}*	1.05±0.004^{d}*	0.94±0.078^{a}*	4.02*
400	1.95±0.004^{a}	1.00±0.003^{a}	0.64±0.068^{bc}	3.59
Sum of sq.	0.149	0.035	0.876	
DF value	59	59	59	
F value	3.867	3.910	3.618	
Sig.	0.005*	0.001*	0.001*	

terpenes, aliphatic, sterols, alcohols, fatty acids, esters, and aldehydes in the leaves of *S. macrophylla* plant and the results indicated that the leaves were a rich source of phytochemicals. A variety of bioactive compounds were detected in the Soxhlet aqueous leaf extract. GC-MS analysis of Soxhlet extract of *S. macrophylla* leaves revealed 21 phytocompounds. The chromatogram and table show the name of phytochemicals, their retention time, peak area, molecular formula, molecular weight of all identified phytocompounds (Figure 8 & Table 7).

ISSR Analysis for the Screening of Mutants

The PCR amplification of control and treated plants DNA was performed with UBC (University of British Columbia) ISSR (Inter Simple Sequence Repeats) universal primers, and the PCR amplified products were detected by agarose gel electrophoresis. Primer UBC 834 showed the significant amplification results of the suspected mutant of *S. macrophylla* plants and control under the same conditions. The amplification products range from different 1 KB to 400 bp and 2 log DNA ladder 3 KB to 100 bp.

The screened ISSR PCR amplified DNA product of the *S. macrophylla* showed increase and deletion of band visualized total 16 bands were amplified, of which 4 were polymorphic bands with a polymorphism ratio of 25% indicating that the test materials were rich in variation. UBC Primer amplified the most polymorphic bands of treated and control (5 treated and 1 control) plants. The materials with primer was shown and some band new more band and deletions. The UBC amplification, material SM 1 was as control have 2 bands (700 and 500 bp) and all bands were counted, band material SM 2 have 2 bands (700 and 500 bp) and material SM 3 have one new more band (1 KB) which was polymorphic band and SM 4 have 1 new more bands (400 bp) which was polymorphic and SM 5 and SM 6 have 1 new bands (1 KB) which was also polymorphic. These polymorphisms were indicated that these numbered plants are as mutants in the NPs treatment (Figure 9).

After identification and analysis of molecular markers, the suspected mutant initially identified by plant morphology had structurally altered phenotype and was tentatively decided as a mutant of *S. macrophylla*.

Flow Cytometric Analysis

The effect of TiO_2 NPs on the ploidy status of *S. macrophylla* plants treated with TiO_2 NPs with different concentrations

Table 7: GC-MS based identification of phytochemicals name of *S. macrophylla* plant treated with 200 mg L^{-1} TiO_2 NPs

Phytochemicals identified (GC-MS)	Retention Time	Peak aria (%)	Molecular weight (g/mol)	Molecular formula
Pyromeconic acid	4.111	0.51	112.08	$C_5H_4O_3$
1-Methyl-2-pyrrolidinone	4.870	0.63	19.13	C_5H_9NO
Pyran-4-one	6.510	0.48	96.08	$C_5H_4O_2$
Sucrose	8.783	0.77	342.30	$C_{12}H_{22}O_{11}$
Quinic acid	10.113	0.56	192.17	$C_7H_{12}O_6$
4-C-Methyl-myo-inositol	10.953	0.72	194.18	$C_7H_{14}O_6$
Scyllo-inositol	11.882	1.21	180.16	$C_6H_{12}O_6$
Methyl elaidolinolenate	14.823	1.38	292.50	$C_{19}H_{32}O_2$
Diethyl benzene-1,2 dicarboxylate	17.675	1.26	444.50	$C_{24}H_{28}O_8$
Hexadecanoic acid	18.711	0.39	256.42	$C_{16}H_{32}O_2$
Myristelaidic acid	20.603	0.83	226.35	$C_{14}H_{26}O_2$
Octadecanoic acid	23.278	0.92	284.50	$C_{18}H_{36}O_2$
Alpha-Linolenic acid	26.789	0.87	278.40	$C_{18}H_{30}O_2$
2-Hexadecen-1-ol	27.985	1.12	240.42	$C_{16}H_{32}O$
Tert-hexadecanethiol	30.110	1.03	969.50	$C_{48}H_{99}AuS_3$
Pentanoic acid	31.597	0.98	102.13	$C_5H_{10}O_2$
4-Pentadecylenol	34.580	1.79	304.50	$C_{21}H_{36}O$
Benzenepropanoic acid	36.931	1.56	150.17	$C_9H_{10}O_2$
Methyl elaidolinolenate	37.993	1.08	292.50	$C_{19}H_{32}O_2$
Stearic acid	45.237	0.84	284.50	$C_{18}H_{36}O_2$
Xanthaurine	46.558	0.75	302.23	$C_{15}H_{10}O_7$

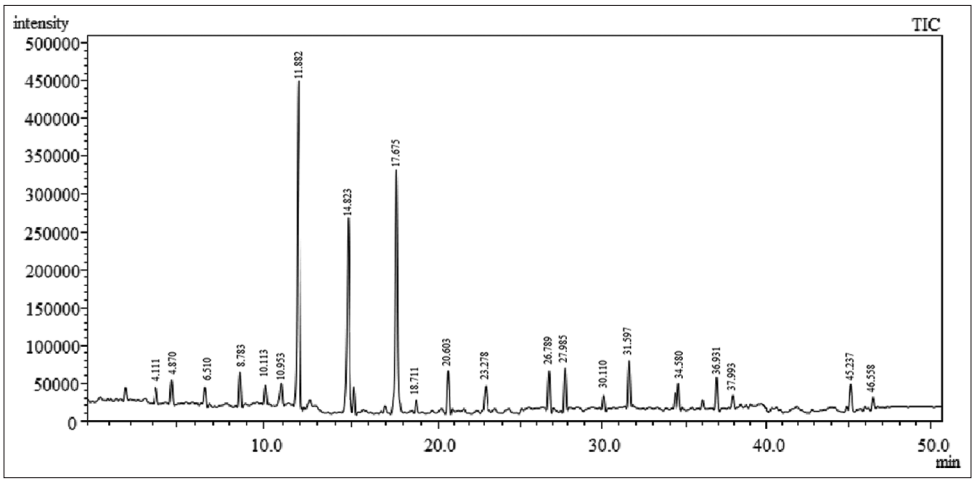

Figure 8: GC-MS chromatogram of leaves extract of *S. macrophylla* plant (120 days old pants) treated with 200 mg L^{-1} of TiO_2 NPs

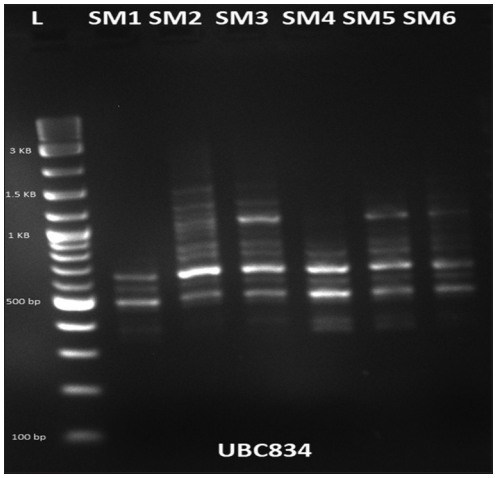

Figure 9: Amplification profile of ISSR primer (UBC 834) L- 2 log DNA ladder, SM1- control, SM2- 25 mg L^{-1}, SM3- 50 mg L^{-1}, SM4- 100 mg L^{-1}, SM5- 200 mg L^{-1}, SM6- 400 mg L^{-1}, treatment of *S. macrophylla* plants

in mg L^{-1} was determined using a flow cytometric analysis in which high-quality nuclei were analyzed. In this research, leaves of *S. macrophylla* plants grown in the field were used as control. The flow cytometric histogram peak of leaves showed that its DNA content was increased by 200 mg L^{-1} TiO_2 NPs treatment, which affected the plants individually. The amount of nuclear DNA in the leaves of treated plants was found to be 0.297 (pg) compared to the leaves DNA 0.280 (pg) of control diploid plants. This flow cytomic analysis of leaves of treated plants confirmed that treatment of TiO_2 NPs increased DNA status in plants (Figure 10).

DISCUSSION

In this research study of *S. macrophylla* an endangered plant species, especially with regard to legally economically important species, require special care to avoid any type of disturbance and harm to local populations. Understanding the

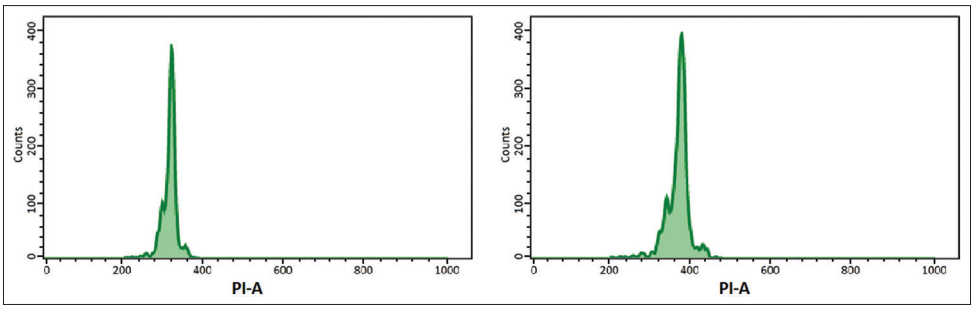

Figure 10: Flow cytometric analyzed graph of ploidy status of *S. macrophylla* plant leaves treated with 200 mg L^{-1} TiO_2 NPs

physio-morphological status of endangered plant populations under natural conditions is essential to understand possible improvement with various environmental abiotic stress conditions.

In this research work UV- Vis spectra of green synthesized TiO_2 NPs showed near 310 nm absorbance wavelength. Rathore *et al.* (2024) reported the UV-Vis spectra of TiO_2 NPs show absorption peak near 394 nm, the absorption peak depends on the morphology and impurities of surface molecules UV-Vis peaks are obtained in the range of 370-400 nm, which depends on the size and shape of synthesized TiO_2 NPs. Girigoswami *et al.* (2024) reported for chemically synthesized TiO_2 NPs the absorption spectrum of NPs was obtained at 261 nm, the UV region of the spectrum (250-400 nm) and the absorption peak of TiO_2 indicated that the synthesized NPs. Vasanth *et al.* (2023) studied morphological properties and size distribution of *Spirulina* mediated titanium dioxide nanoparticles were studied using diffraction of laser light source Green synthesis of titanium dioxide nanoparticles Zeta potential was 20 nm. Kushwah and Patel (2019) reported the distribution was calculated with the intensity variations within the diffraction pattern at the initial state and the particle size distribution of the TiO_2 synthesized nanoparticles was evaluated from 60 to 300 nm.

This research study FTIR spectrum of plant based synthesized TiO_2 NPs indicated the broad peak at 1628.43 cm^{-1} which was represent the synthesized fictional group of NPs. Bopape *et al.* (2023) reported in the Infrared spectrum of TiO_2 NPs from *C. bengalensis* plant leaves extract, an intense band was at 1641 cm^{-1} observed. It corresponds to the amide band, which arises due to the carbonyl stretching and N–H deformation vibration in the amide linkage of *C. bengalensis* protein. Rathi and Jeice (2023) reported that The FTIR of TiO_2 NPs revealed the presence of many functional groups at various wavelengths in the 4000-400 cm^{-1} range. The large absorption peak, at 3831 and 3751 cm^{-1}, indicated presence of alcohols, phenols including O-H stretches. the prominent peak at 2174 and 2020 cm^{-1} showed aliphatic amines with C-N stretching, the signal vibration at 1062 cm^{-1}indicated presence of O-Ti-O indicated the presence of TiO_2 NPs. Sowmya *et al.* (2023) reported potential functional groups, of leaf extracts of *Alternanthera sessilis* indicate the broad absorption peak at 3435.89 cm^{-1} represent to O-H bending (alcohol and phenol). The peak spectra at 1643.69.83 cm^{-1} indicate C-O stretch (ether groups), the absorption peaks at 1033.90 cm^{-1}, 691.76 cm^{-1}, and 1643.69 cm^{-1} responsible for presence of amines, aliphatic and aromatic which showed bio-reduction of synthesized TiO_2 NPs.

The present research XRD pattern was indicate the green synthesized TiO_2 NPs formed in crystalline and anatase phase. The TiO_2 was identified by the diffraction peaks characteristic at different theta ranges 25.3° (101), 36.9° (103), 37.8° (004), 48.05° (200), 53.9° (105), 62.12° (213), 68.7° (116), 70.311° (220), 75.03° (215), and 76.02° (301) corresponding plans to anatase phase of TiO_2 (JCPDS card no. 21-1272) (Gou & Guo, 2019). The XRD pattern of the TiO_2 NPs was calcinated at 500 °C for 5 h to form anatase phase. The diffraction peaks pattern (JCPDS card no. 21-1272). The peak position was observed at 25.3°, 37.8°, 48.0°, 53.9°, 55.0°, 62.7° 68.77° and 75.49° corresponds to the planes (101), (004), (200), (105), (211), (204), (116) and (215) respectively (Kumar *et al.*, 2023). The peaks of XRD pattern at 101, 103, 004, 112, 200, 105, 211, 204, 116, and 215 that indicate anatase structure (JCPDS card no. 89-4921) (Girigoswami *et al.*, 2024).

The SEM micrograph analysis of synthesized TiO_2 NPs showed the spherical structure and oval morphology with 75 nm sizes of NPs. Bazzanella *et al.* (2023) reported the SEM topology shows that TiO_2 consists of small particles ranging from 10-20 nm, which was spherical and oval in shape. SEM study indicated the synthesized NPs were triangular-shaped and the average size was 153.4 nm, the energy band gap was 3.13 eV of synthesized TiO_2 NPs (Saini & Kumar, 2023). The surface topology of TiO_2 NPs was analyzed using SEM micrographs of NPs find diameter of 200 nm, several structures such as irregular spheres, pentagons, and hexagons of NPs. The SEM topology of spherical-like morphology of the TiO_2 NPs synthesized using *Azadirechta indica* plant leaves extracts. Various interactions during synthesis with metal precursors affect the nucleation of TiO_2 NPs (Rana *et al.*, 2024). SEM micrograph images of ZnO NPs it exhibit agglomeration of oval and spherical grains structure (Gemachu & Birhanub, 2024).

In the present research study effects of plant based synthesized TiO_2 NPs on seed germination, growth rate of root and shoot, seedling growth rate parameter at different time duration, plant development in natural condition, chlorophylls pigment analysis of all plants, phytochemicals quantification in treated plant leaves and ploidy status of the certain affected plants, these parameters improved through impact of NPs. The photo catalytic activity of synthesized TiO_2 NPs positively affected

germination rate of seeds and growth differences via gibberellins pathway in the plants (Wang *et al.*, 2021). Nanoparticles significantly promote root and shoot growth Poaceae plants, increase chlorophyll content, enhance resistance to external environmental stresses, NPs can cause oxidative stress, affect plant photosynthesis and chlorophyll content, and influence plant physiological and biochemical responses (Li *et al.*, 2024). Application of TiO_2 NPs through the leaf resulted in increased fruit yield and individual fruit weight, increased fruit size, as measured by polar and equatorial diameters (Pérez-Velasco *et al.*, 2023). The sprayed TiO_2 NPs bio accumulated in the tissues of all tomato plant parts and TiO_2 NPs were mainly sprayed on leaves for 7 days. Analysis of detached tomato leaves showed that the NPs enhanced the resistance of tomato plants to wilt disease (Pan *et al.*, 2023). The synthesized NPs improved seedling growth parameters as well as phytochemical components; Cu-Ag NPs enhanced plant height, antioxidant capacity, biochemical synthesis (Mawale *et al.*, 2024). Application of magnetite NPs suspension with 100 ppm improved the morphological and physiological parameters of plants (Velásquez *et al.*, 2024).

The optimal concentration of Fe_3O_4 NPs, 10 and 50 mg L^{-1} was enhanced seed germination, growth rate, chlorophyll pigment of tomato seedlings compared to control (Singh *et al.*, 2024). ZnO-NPs enhance antioxidant and nutrient absorption during NaCl stress conditions, resulting in enhanced root system growth and improved plant adaptability and salinity tolerance (Singh *et al.*, 2022). Effects of plant based synthesized NPs on rice seed germination, biochemical, morpho-physiological, enhanced nutrient status compared with natural materials and benefits to agriculture sector (Setty *et al.*, 2023). SiO_2-NPs enhanced the photosynthesis rate of cotton plants and improved the electron transport activity of PSII, and also increased the Rubisco activity during low temperature and salt stress at 100 mg L^{-1} NPs (Liang *et al.*, 2023). The essential wood oil of *S. macrophylla* was separated by hydro distillation unit and analyzed with GC-MS. The oil contained sesquiterpene hydrocarbons 65.9%, oxygenated sesquiterpenoids 29.6%, cadinene 33.0%, α-copaene 7.2%, α-cadinol 7.1%, τ-murolol 6.1% and τ-cadinol 4.5%, respectively (Suarez *et al.*, 2019). The DNA content is analyzed by flow cytometry, which allows the analysis of a large number of nucleated cells. A large number of samples have to be processed and double haploid techniques are produced by breeding polyploid species (Fomicheva & Domblides, 2023). The new limonoids 1, 2 and 3 evaluated for anti-inflammatory, antimicrobial, genotoxic and hemolytic properties in plants. Biocompounds have hypoglycemic activity and which was used for the controlling of blood sugar levels and diabetes and also antibacterial activity. The therapeutic impact of limonoids isolated from *S. macrophylla* help in potential new drugs (Asokan *et al.*, 2024).

CONCLUSION

The present study describes a cost-effective and eco-friendly green synthesis of TiO_2 NPs using aqueous extract of *Lantana camara* L. plant as reducing, capping and stabilizing agent. The NPs were characterized using UV-Vis spectroscopy, FTIR, SEM, XRD and PSA analytical techniques. The UV–Vis spectra revealed a band at 310 nm which was responsible for the confirmation of TiO_2 NPs. FTIR analysis showed the presence of secondary metabolites in the extract, which were responsible for reducing and capping the ion into NPs with characteristic stretching vibration at 522 cm^{-1}. SEM micrographs confirmed that the surface topology was spherical shape of NPs. X-ray diffraction analysis confirmed the crystalline nature and anatase TiO_2 NPs, and the PSA was calculated with an average size 75 nm of the NPs. The research showed that TiO_2 NPs had effects on seed germination, root and shoot growth, plant length, number of leaves on different days, which significantly increased the germination, survival ability, and root, shoot, and leaf length of the endangered plant species *S. macrophylla*. The positive effect of TiO_2 NPs resulted in significant increase in photosynthetic pigments. GC-MS analysis identified 21 phytochemicals that are beneficial for traditional medicine. The ISSR results confirmed the polymorphism and induction of mutants in the treated plants. The ploidy status of leaves of treated plants also increased the DNA content in plants, a finding confirming that TiO_2 NPs highly affected the growth parameters and DNA status of endangered plants.

ACKNOWLEDGEMENT

The authors are thankful to Central Instrumentation Facility (CIF) Jiwaji University, Gwalior for providing available facilities of this research work.

AUTHORS' CONTRIBUTIONS

DKV designed plan of research work, synthesized nanoparticles and perform all experimental work, ABT supervised and provide most valuable suggestions, SP wrote the manuscript together with DKV and help in statistical analysis of the data.

REFERENCES

Asokan, K., Hussain, A. Z., Gattu, R. K., & Ilangovan, A. (2024). Minor limonoid constituents from *Swietenia macrophylla* by simultaneous isolation using supercritical fluid chromatography and their biological activities. *RSC Advances, 14*(36), 26637-26647. https://doi.org/10.1039/D4RA03663H

Bazzanella, N., Bajpai, O. P., Fendrich, M., Guella, G., Miotello, A., & Orlandi, M. (2023). Ciprofloxacin degradation with a defective TiO_{2-x} nanomaterial under sunlight. *MRS Communications, 13*, 1252-1259. https://doi.org/10.1557/s43579-023-00440-4

Bopape, D. A., Mathobela, S., Matinise, N., Motaung, D. E., & Hintsho-Mbita, N. C. (2023). Green synthesis of CuO-TiO_2 nanoparticles for the degradation of organic pollutants: physical, optical and electrochemical properties. *Catalysts, 13*(1), 163. https://doi.org/10.3390/catal13010163

Cardoso, V. S. L., Valente-Amaral, A., Monteiro, R. F. M., Meira, C. L. S., de Meira, N. S., da Silva, M. N., Pinheiro, J. de J. V., Bastos, G. de N. T., Felício, J. S., & Yamada, E. S. (2024). Aqueous extract of *Swietenia macrophylla* leaf exerts an anti-inflammatory effect in a murine model of Parkinson's disease induced by 6-OHDA. *Frontiers in Neuroscience, 18*, 1351718. https://doi.org/10.3389/fnins.2024.1351718

Chandren, S., & Rusli, R. (2022). Biosynthesis of TiO_2 nanoparticles and their application as catalyst in biodiesel production. In M. Srivastava, M. A. Malik, & P. K. Mishra (Eds.), *Green Nano Solution*

for Bioenergy Production Enhancement (pp. 127-168) Singapore: Springer. https://doi.org/10.1007/978-981-16-9356-4_6

Falcioni, R., Antunes, W. C., Demattê, J. A. M., & Nanni, M. R. (2023). A novel method for estimating chlorophyll and carotenoid concentrations in leaves: A two hyperspectral sensor approach. *Sensors, 23*(8), 3843. https://doi.org/10.3390/s23083843

Fomicheva, M., & Domblides, E. (2023). Mastering DNA content estimation by flow cytometry as an efficient tool for plant breeding and biodiversity research. *Methods and Protocols, 6*(1), 18. https://doi.org/10.3390/mps6010018

Gemachu, L. Y., & Birhanu, A. L. (2024). Green synthesis of ZnO, CuO and NiO nanoparticles using neem leaf extract and comparing their photocatalytic activity under solar irradiation. *Green Chemistry Letters and Reviews, 17*(1), 2293841. https://doi.org/10.1080/17518253.2023.2293841

Girigoswami, A., Deepika, B., Pandurangan, A. K., & Girigoswami, K. (2024). Preparation of titanium dioxide nanoparticles from *Solanum Tuberosum* peel extract and its applications. *Artificial Cells, Nanomedicine, and Biotechnology, 52*(1), 59-68. https://doi.org/10.1080/21691401.2023.2301068

Gou, X., & Guo, Z. (2019). Hybrid hydrophilic–hydrophobic CuO@TiO_2-coated copper mesh for efficient water harvesting. *Langmuir, 36*(1), 64-73. https://doi.org/10.1021/acs.langmuir.9b03224

Huang, Y., Dong, Y., Ding, X., Ning, Z., Shen, J., Chen, H., & Su, Z. (2022). Effect of nano-TiO_2 composite on the fertilization and fruit-setting of litchi. *Nanomaterials, 12*(23), 4287. https://doi.org/10.3390/nano12234287

Jaime, A. B., González, R. M., Rosales, D. H., Verdín, E. M. B., González, E. M., Noriega, R. P., González, A. M., & Morales, J. R. F. (2024). Effect of *Swietenia macrophylla* king and *Eriobotrya japonica* lindl on clinic biochemistry of hyperglycemic Wistar rats. *South Florida Journal of Development, 5*(2), 580-591. https://doi.org/10.46932/sfjdv5n2-013

Kumar, S., Dwivedi, A., Pandey, A. K., & Vajpayee, P. (2023). TiO_2 nanoparticles alter nutrients acquisition, growth, biomacromolecules, oil composition and modulate antioxidant defense system in *Mentha arvensis* L. *Plant Nano Biology, 3*, 100029. https://doi.org/10.1016/j.plana.2023.100029

Kushwah, K. S., & Patel, S. (2020). Effect of titanium dioxide nanoparticles (TiO 2 NPs) on Faba bean (*Vicia faba* L.) and induced asynaptic mutation: a meiotic study. *Journal of Plant Growth Regulation, 39*, 1107-1118. https://doi.org/10.1007/s00344-019-10046-7

Kushwah, K. S., & Verma, D. K. (2021). Biological synthesis of metallic nanoparticles from different plant species. In P. V. Pham (Eds.), *21st century nanostructured materials-physics, chemistry, classification, and emerging applications in industry, biomedicine, and agriculture* London, UK: IntechOpen Limited. https://doi.org/10.5772/intechopen.101355

Kushwah, K. S., Patel, S., & Verma, D. K. (2022). Synthesis and effect of TiO_2 nanoparticles on phytotoxicity and genotoxicity in *Pisum sativum* L. *Vegetos, 35*, 204-211. https://doi.org/10.1007/s42535-021-00236-8

Li, P., Xia, Y., Song, K., & Liu, D. (2024). The Impact of nanomaterials on photosynthesis and antioxidant mechanisms in gramineae plants: Research progress and future prospects. *Plants, 13*(7), 984. https://doi.org/10.3390/plants13070984

Li, Y., Chen, L., Zhan, X., Liu, L., Feng, F., Guo, Z., Wang, D., & Chen, H. (2022). Biological effects of gamma-ray radiation on tulip (*Tulipa gesneriana* L.). *PeerJ, 10*, e12792. https://doi.org/10.7717/peerj.12792

Li, Y., Cheng, X., Lai, J., Zhou, Y., Lei, T., Yang, L., Li, J., Yu, X., & Gao, S. (2023). ISSR molecular markers and anatomical structures can assist in rapid and directional screening of cold-tolerant seedling mutants of medicinal and ornamental plant in *Plumbago indica* L. *Frontiers in Plant Science, 14*, 1149669. https://doi.org/10.3389/fpls.2023.1149669

Liang, Y., Liu, H., Fu, Y., Li, P., Li, S., & Gao, Y. (2023). Regulatory effects of silicon nanoparticles on the growth and photosynthesis of cotton seedlings under salt and low-temperature dual stress. *BMC Plant Biology, 23*, 504. https://doi.org/10.1186/s12870-023-04509-z

Mawale, K. S., Nandini, B., & Giridhar, P. (2024). Copper and silver nanoparticle seed priming and foliar spray modulate plant growth and thrips infestation in *Capsicum* spp. *ACS Omega, 9*(3), 3430-3444. https://doi.org/10.1021/acsomega.3c06961

Metwally, R. A., El Nady, J., Ebrahim, S., El Sikaily, A., El-Sersy, N. A., Sabry, S. A., & Ghozlan, H. A. (2023). Biosynthesis, characterization and optimization of TiO_2 nanoparticles by novel marine halophilic *Halomonas* sp. RAM2: application of natural dye-sensitized solar cells. *Microbial Cell Factories, 22*, 78. https://doi.org/10.1186/s12934-023-02093-3

Pan, X., Nie, D., Guo, X., Xu, S., Zhang, D., Cao, F., & Guan, X. (2023). Effective control of the tomato wilt pathogen using TiO_2 nanoparticles as a green nanopesticide. *Environmental Science: Nano, 10*(5), 1441-1452.

Pérez-Velasco, E. A., Valdez-Aguilar, L. A., Betancourt-Galindo, R., González-Fuentes, J. A., & Baylón-Palomino, A. (2023). Covered rutile-TiO_2 nanoparticles enhance tomato yield and growth by modulating gas exchange and nutrient status. *Plants, 12*(17), 3099. https://doi.org/10.3390/plants12173099

Pulit-Prociak, J., Długosz, O., Staroń, A., Radomski, P., Domagała, D., & Banach, M. (2023). *In vitro* studies of titanium dioxide nanoparticles modified with glutathione as a potential drug delivery system. *Nanotechnology Reviews, 12*(1), 20230126. https://doi.org/10.1515/ntrev-2023-0126

Pyne, S., & Paria, K. (2022). Optimization of extraction process parameters of caffeic acid from microalgae by supercritical carbon dioxide green technology. *BMC chemistry, 16*, 31. https://doi.org/10.1186/s13065-022-00824-y

Rana, A., Pathak, S., Kumar, K., Kumari, A., Chopra, S., Kumar, M., Kamil, D., Srivastava, R., Kim, S.-K., Verma, R., & Sharma, S. N. (2024). Multifaceted properties of TiO 2 nanoparticles synthesized using *Mangifera indica* and *Azadirachta indica* plant extracts: antimicrobial, antioxidant, and non-linear optical activity investigation for sustainable agricultural applications. *Materials Advances, 5*(7), 2767-2784. https://doi.org/10.1039/D3MA00414G

Rathi, V. H., & Jeice, A. R. (2023). Green fabrication of titanium dioxide nanoparticles and their applications in photocatalytic dye degradation and microbial activities. *Chemical Physics Impact, 6*, 100197. https://doi.org/10.1016/j.chphi.2023.100197

Rathore, C., Yadav, V. K., Amari, A., Meena, A., Egbosiuba, T. C., Verma, R. K., Mahdhi, N., Choudhary, N., Sahoo, D. K., Chundawat, R. S., & Patel, A. (2024). Synthesis and characterization of titanium dioxide nanoparticles from *Bacillus subtilis* MTCC 8322 and its application for the removal of methylene blue and orange G dyes under UV light and visible light. *Frontiers in Bioengineering and Biotechnology, 11*, 1323249. https://doi.org/10.3389/fbioe.2023.1323249

Rathore, C., Yadav, V. K., Gacem, A., AbdelRahim, S. K., Verma, R. K., Chundawat, R. S., Gnanamoorthy, G., Yadav, K. K., Choudhary, N., Shaoo, D. K., & Patel, A. (2023). Microbial synthesis of titanium dioxide nanoparticles and their importance in wastewater treatment and antimicrobial activities: a review. *Frontiers in Microbiology, 14*, 1270245. https://doi.org/10.3389/fmicb.2023.1270245

Sagadevan, S., Imteyaz, S., Murugan, B., Lett, J. A., Sridewi, N., Weldegebrieal, G. K., Fatimah, I., & Oh, W.-C. (2022). A comprehensive review on green synthesis of titanium dioxide nanoparticles and their diverse biomedical applications. *Green Processing and Synthesis, 11*(1), 44-63. https://doi.org/10.1515/gps-2022-0005

Sahu, S. K., Liu, M., Wang, G., Chen, Y., Li, R., Fang, D., Sahu, D. N., Mu, W., Wei, J., Liu, J., Zaho, Y., Zhang, S., Lisby, M., Liu, X., Xu, X., Li, L., Wang, S., Liu, H., & He, C. (2023). Chromosome-scale genomes of commercially important mahoganies, *Swietenia macrophylla* and *Khaya senegalensis*. *Scientific Data, 10*, 832. https://doi.org/10.1038/s41597-023-02707-w

Saini, R., & Kumar, P. (2023). Green synthesis of TiO_2 nanoparticles using *Tinospora cordifolia* plant extract & its potential application for photocatalysis and antibacterial activity. *Inorganic Chemistry Communications, 156*, 111221. https://doi.org/10.1016/j.inoche.2023.111221

Sampayo-Maldonado, S., Ordoñez-Salanueva, C. A., Mattana, E., Way, M., Castillo-Lorenzo, E., Dávila-Aranda, P. D., Lira-Saade, R., Téllez-Valdés, O., Rodriguez-Arevalo, N. I., Ulian, T., & Flores-Ortíz, C. M. (2021). Thermal niche for seed germination and species distribution modelling of *Swietenia macrophylla* king (mahogany) under climate change scenarios. *Plants, 10*(11), 2377. https://doi.org/10.3390/plants10112377

Selvakesavan, R. K., Kruszka, D., Shakya, P., Mondal, D., & Franklin, G. (2023). Impact of nanomaterials on plant secondary metabolism. In J. M. Al-Khayri, L. M. Alnaddaf & S. M. Jain (Eds.), *Nanomaterial interactions with plant cellular mechanisms and macromolecules and agricultural implications* (pp. 133-170) Cham, Switzerland: Springer.

https://doi.org/10.1007/978-3-031-20878-2

Setty, J., Samant, S. B., Yadav, M. K., Manjubala, M., & Pandurangam, V. (2023). Beneficial effects of bio-fabricated selenium nanoparticles as seed nanopriming agent on seed germination in rice (*Oryza sativa* L.). *Scientific Reports, 13*, 22349. https://doi.org/10.1038/s41598-023-49621-0

Singh, A., Sengar, R. S., Shahi, U. P., Rajput, V. D., Minkina, T., & Ghazaryan, K. A. (2022). Prominent effects of zinc oxide nanoparticles on roots of rice (*Oryza sativa* L.) grown under salinity stress. *Stresses, 3*(1), 33-46. https://doi.org/10.3390/stresses3010004

Singh, N., Singh, M. K., Raghuvansi, J., Yadav, R. K., & Azim, Z. (2024). Green synthesis of nano iron oxide using *Emblica officinalis* L. fruit extract and its impact on growth, chlorophyll content, and metabolic activity of *Solanum lycopersicum* L. *Journal of Applied Biology & Biotechnology, 12*(2), 173-181. https://doi.org/10.7324/JABB.2024.165651

Sowmya, M., Puttaswamy, A. A., Prasad, H. S. N., Geetha, N., Girija S., & Venkatachalam, P. (2023). Biogenic Synthesis of *Alternanthera Sessilis* Titanium Dioxide Nanoparticles (AS@TiO_2NP's): A Potential Contender against Perilous Pathogens and Catalytic Degradation of Organic Dyes. *Biointerface Research in Applied Chemistry, 13*(5), 462.

Suarez, A. V., Satyal, P., & Setzer, W. N. (2019). The wood essential oil composition of *Swietenia macrophylla* from Guanacaste, Costa Rica. *American Journal of Essential Oils and Natural Products, 7*(1), 14-16.

Vasanth, V., Murugesh, K. A., Tilak, M., Aruna, R., Raj, P. M., & Arasakumar, E. (2023). Green synthesis of *Spirulina* mediated titanium dioxide nanoparticles and their characterization. *Journal of Survey in Fisheries Sciences, 10*(3), 21-27.

Velásquez, A. A., Urquijo, J. P., Montoya, Y. A., Susunaga, D. M., & Villanueva-Mejía, D. F. (2024). Evaluation of the application of suspensions of iron oxide magnetic nanoparticles functionalized with quaternized chitosan and phosphates on yellow maize and chili pepper plants. *Interactions, 245*, 27. https://doi.org/10.1007/s10751-024-01843-y

Verma, D. K., Patel, S., & Kushwah, K. S. (2020a). Green biosynthesis of silver nanoparticles and impact on growth, chlorophyll, yield and phytotoxicity of *Phaseolus vulgaris* L. *Vegetos, 33*, 648-657. https://doi.org/10.1007/s42535-020-00150-5

Verma, D. K., Patel, S., & Kushwah, K. S. (2020b). Synthesis of titanium dioxide (TiO_2) nanoparticles and impact on morphological changes, seeds yield and phytotoxicity of *Phaseolus vulgaris* L. *Tropical Plant Research, 7*(1), 158-170. https://doi.org/10.22271/tpr.2020.v7.i1.021

Verma, D. K., Patel, S., & Kushwah, K. S. (2021). Effects of nanoparticles on seed germination, growth, phytotoxicity and crop improvement. *Agricultural Reviews, 42*(1), 1-11. https://doi.org/10.18805/ag.R-1964

Verma, S. K., Kumar, P., Mishra, A., Khare, R., & Singh, D. (2024). Green nanotechnology: illuminating the effects of bio-based nanoparticles on plant physiology. *Biotechnology for Sustainable Materials, 1*, 1. https://doi.org/10.1186/s44316-024-00001-2

Wang, C.-J., Zhang, Z.-X., & Wan, J.-Z. (2019). Vulnerability of global forest ecoregions to future climate change. *Global Ecology and Conservation, 20*, e00760. https://doi.org/10.1016/j.gecco.2019.e00760

Wang, J., Li, M., Feng, J., Yan, X., Chen, H., & Han, R. (2021). Effects of TiO_2-NPs pretreatment on UV-B stress tolerance in *Arabidopsis thaliana*. *Chemosphere, 281*, 130809. https://doi.org/10.1016/j.chemosphere.2021.130809

Yitagesu, G. B., Leku, D. T., & Workneh, G. A. (2023). Green synthesis of TiO_2 using *Impatiens rothii* Hook. f. leaf extract for efficient removal of methylene blue dye. *ACS Omega, 8*(46), 43999-44012. https://doi.org/10.1021/acsomega.3c06142